chemistry proceedings

MDPI

Proceeding Paper

MOF-Based Composites for Sustainable Processes †

Marzia Pentimalli [1,*], Stefano De Antonellis [2], Alessandra Fava [1], Cristina Stifani [1] and Franco Padella [3]

[1] Department for Sustainability, Casaccia Research Centre, ENEA Italian National Agency for Energy, New Technologies and Sustainable Economic Development, Via Anguillarese 301, 00123 Rome, Italy; alessandra.fava@enea.it (A.F.); cristina.stifani@enea.it (C.S.)
[2] Department of Energy, Campus Bovisa, Politecnico di Milano, Via Lambruschini 4a, 20156 Milan, Italy; stefano.deantonellis@polimi.it
[3] Independent Researcher, 00100 Rome, Italy; fpadella@gmail.com
* Correspondence: marzia.pentimalli@enea.it; Tel.: +39-06-3048-3254
† Presented at the 5th International Online Conference on Crystals, 15–17 June 2026; Available online: https://sciforum.net/event/IOCC2026.

Abstract

Metal–Organic Frameworks (MOFs) are hybrid crystalline materials with exceptional adsorption properties, but their powdered form can hinder practical implementation. Mixed Matrix Membranes (MMMs) embedding active particles in a polymer matrix combine MOF performance with mechanical robustness. We report on an Al-fumarate/PVDF-HFP MMM (67 wt% MOF loading) prepared by solution casting. The MOF in the membrane retains ~90% of its pristine specific surface area, exhibits the characteristic Type V water adsorption isotherm of Al-fumarate with negligible hysteresis and outperforms conventional silica gel under representative heat-driven dehumidification in air-conditioning operating conditions. The hydrophobic PVDF-HFP prevents water accumulation, preserving MOF active sites. The membrane addresses powder handling limitations, representing a key step towards MOF integration into HVAC and dehumidification systems.

Keywords: metal–organic framework; mixed matrix membrane; Al-fumarate; PVDF-HFP; water adsorption; HVAC

1. Introduction

Metal–Organic Frameworks (MOFs) are hybrid crystalline materials with ultrahigh surface areas, tunable pore sizes and versatile chemical functionalities [1,2]. They have attracted interest in applications from gas storage and separation [3,4] to catalysis [5], water treatment [6], chemical sensing [7], food packaging [8], batteries [9] and drug delivery [10]. Among MOFs, aluminum fumarate (Al-fumarate) is particularly promising for water adsorption due to its Type V isotherm and low hysteresis, enabling efficient uptake and release with minimal energy input [11], properties ideal for dehumidification, water recovery, passive cooling, and heat transformation processes [12,13].

As-synthesized MOFs are fine powders, posing challenges for real devices: difficult handling, particle dispersion, high pressure drops in devices and poor mechanical stability. This has motivated research into shaping MOFs into pellets, foams, monoliths or composites [14]. Mixed Matrix Membranes (MMMs)—high loadings of particulate bound in a polymer matrix—combine MOF adsorption with mechanical robustness, flexibility and processability, yielding free-standing films that can be easily handled and integrated [15].

The need for advanced desiccants is acute in Heating, Ventilation, and Air Conditioning (HVAC), where dehumidification drives energy consumption. Adsorption-based

Check for updates

Academic Editor: Ferdinando Costantino

Published: 8 October 2026

Copyright: © 2026 by the authors. Licensee MDPI, Basel, Switzerland. This article is an open access article distributed under the terms and conditions of the Creative Commons Attribution (CC BY) license.

systems can exploit low-grade thermal sources (e.g., solar or waste heat) rather than electricity, offering primary energy savings [16]. Conventional silica gel has limited capacity and requires relatively high regeneration temperatures [16]; MOFs with tailored pores and high uptake can overcome these limits.

Previously, Al-fumarate powder showed a ~50% reduction in thermal energy demand in pilot-scale pasta-drying tests [11,12], but powder dispersion and pressure drops hindered practical deployment. The present work addresses these limitations by developing an Al-fumarate/PVDF-HFP MMM. The hydrophobic, chemically stable copolymer PVDF-HFP was chosen for its compatibility with various processing techniques [17]. The membrane can enable a fixed-bed desiccant module to be integrated into HVAC and drying systems. This work provides a novel demonstration that a high-loading Al-fumarate/PVDF-HFP MMM can retain the intrinsic adsorption properties of the MOF while enabling easy handling and integration, and benchmarks its performance against silica gel under HVAC-relevant conditions. The paper reports the development and characterization of the MMM at the 67 wt% MOF loading, already identified as an optimal composition [18]. The 67 wt% MOF loading was identified as optimal in our previous work, because it provides the best compromise between high MOF surface area retention (~90%) and sufficient polymer content for mechanical integrity, whereas lower loadings suffer from pore occlusion by the polymer and higher loadings lead to particle aggregation and brittle membranes [18].

2. Materials and Methods

Al-fumarate MOF was purchased from MOFTechnologies Ltd., Belfast, UK (CAS 132041-53-3; MW = 158.05 g/mol) and used as received. PVDF-HFP copolymer (CAS 9011-17-0; Mn = 130,000, Mw = 400,000) was acquired from Sigma-Aldrich, St. Louis, MO, USA. Dimethylformamide (DMF, 100%, VWR Chemicals, Radnor, PA, USA) was used as the solvent. The Al-fumarate/PVDF-HFP MMM was prepared by solution casting following the protocol already described in our previous work [18]. Briefly, a 10% *w*/*w* PVDF-HFP solution was prepared by dissolving the polymer pellets in DMF at 70 °C under stirring for 3 h. The Al-fumarate MOF was then added to achieve a 67 wt% final loading. The slurry was homogenized by mechanical mixing, cast onto a glass substrate and dried at room temperature for 12 h, yielding a free-standing membrane with a thickness of 200–400 µm. ATR-FTIR spectra were acquired using a Thermo Fisher, Waltham, MA, USA Nicolet 6700 spectrometer, equipped with a Specac Golden Gate ATR, Orpington, UK, unit with a diamond internal reflection element (IRE) set at 45°. Each spectrum resulted from the co-addition of 64 scans, recorded at a 4 cm^{-1} resolution. Spectra were collected on the pristine materials (Al-fumarate powder and PVDF-HFP pellets), on a neat PVDF-HFP film cast from DMF, and on the M67 composite membrane. XRD patterns were collected using a Rigaku Smartlab, Tokyo, Japan, diffractometer (Cu-Kα radiation). To confirm the preservation of crystal parameters of the MOF structure, XRD data were refined by the Rietveld method, using the MAUD software, version 2.999 (https://maud.radiographema.eu, accessed on 19 July 2026) [19]. SEM analysis was performed using a ZEISS LEO 1530, Oberkochen, Germany, instrument. Nitrogen adsorption isotherms at 77 K were collected using an Autosorb iQ30 instrument (Quantachrome, Boynton Beach, FL, USA) after 8 h outgassing at 100 °C. Specific surface areas were calculated using the BET equation; pore size distributions in the micropore range were obtained using the Horvath–Kawazoe (HK) model, while the Barrett–Joyner–Halenda (BJH) model was applied to evaluate the mesoporosity. Static contact angle measurements were performed by depositing 5 µL water droplets on the membrane surface and acquiring images over time using Motic Image Plus 2.0 software (Motic, Hong Kong, China). At least five droplets were analyzed per sample, and the average value is reported. Water vapor adsorption/desorption isotherms were measured

using an Aquadyne DVS2 dynamic vapor sorption system. Water vapor sorption isotherms were recorded on an Aquadyne DVS2 analyzer. About 45 mg of sample was used with a total gas flow of 100 sccm (standard cubic centimeters per minute). Prior to measurement, the sample was preconditioned via several adsorption–desorption cycles between 5 and 80% RH. The protocol included drying at 85 °C under nitrogen for 12 h, and then conditioning at 50 °C. Relative humidity was increased stepwise with finer steps between 16 and 40% RH to resolve the S-shaped isotherm. Each step had a minimum duration of 180 min and a maximum of 500 min, and equilibrium was assumed when the mass-change rate fell below 0.001% min^{-1}. Typical HVAC operating conditions were selected for the comparison with silica gel (process air at 30 °C, 40% RH; regeneration air at 70 °C, 10% RH). Silica gel was selected as the benchmark because it is the most widely used desiccant in HVAC systems.

3. Results and Discussion

3.1. The MMM Material Structure and Morphology

ATR-FTIR analysis was performed to investigate possible chemical interactions between Al-fumarate and PVDF-HFP in the composite membranes (Figure 1A). The spectrum of the pristine PVDF-HFP pellets shows the characteristic absorption bands of the α-phase at 613, 762, and 975 cm^{-1}. Upon casting from DMF solution, the polymer film undergoes a transition to the β-polymorph, evidenced by the disappearance of the α-phase bands and the appearance of a prominent band at 840 cm^{-1} accompanied by a shoulder at 1275 cm^{-1} [20]. Notably, the spectrum of the M67 membrane is a simple superposition of the β-phase PVDF-HFP bands and the MOF absorptions, with all spectral features perfectly preserved—strongly suggesting that no appreciable chemical interaction occurs between the two components. The preservation of the MOF crystalline structure within the polymer matrix was checked by XRD analysis (Figure 1B). The M67 membrane exhibits the characteristic reflections of pristine Al-fumarate, with the main (011) peak at about 10.4° 2θ, and no additional peaks or shifts are observed—indicating that the MOF structure remains intact during processing. Rietveld refinement confirmed that the lattice parameters are maintained within ±0.5% variation, with no significant microstructural distortion (grain size ~290 Å, microstrain < 0.007).

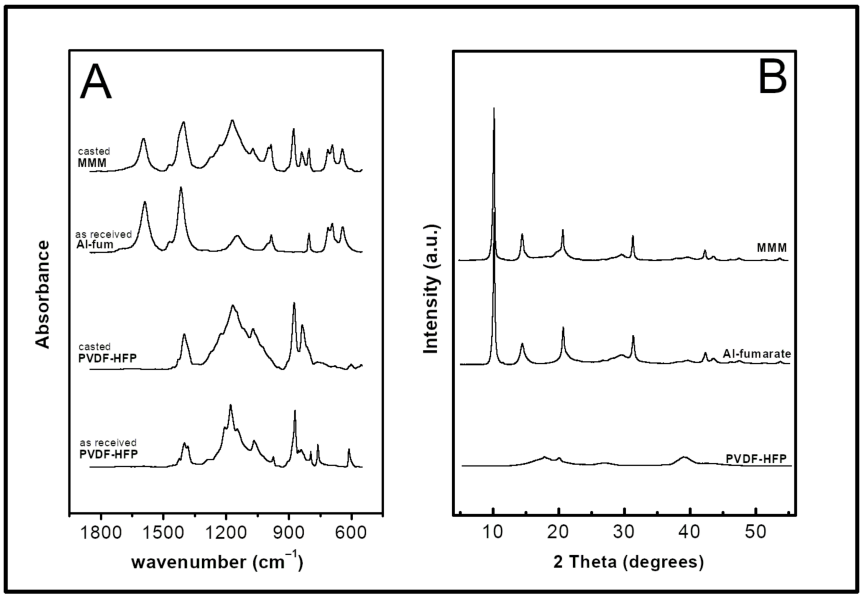

Figure 1. (**A**) ATR-FTIR spectra of pristine Al-fumarate, PVDF-HFP film (as received and cast from DMF) and M67 composite membrane; (**B**) XRD patterns of pristine Al-fumarate, PVDF-HFP and M67 membrane.

SEM analysis (Figure 2) reveals a porous and irregular surface morphology typical of films obtained by solvent casting, with micrometric porosity due to solvent evaporation. The inset shows the pristine Al-fumarate material, which consists of spherical aggregates of fine needle-like crystals. The M67 membrane also exhibits good mechanical stability and handling properties, as detailed in our previous work [18]; it can be easily cut and modeled without fracturing, confirming the suitability of the PVDF-HFP matrix as a support for the MOF particles.

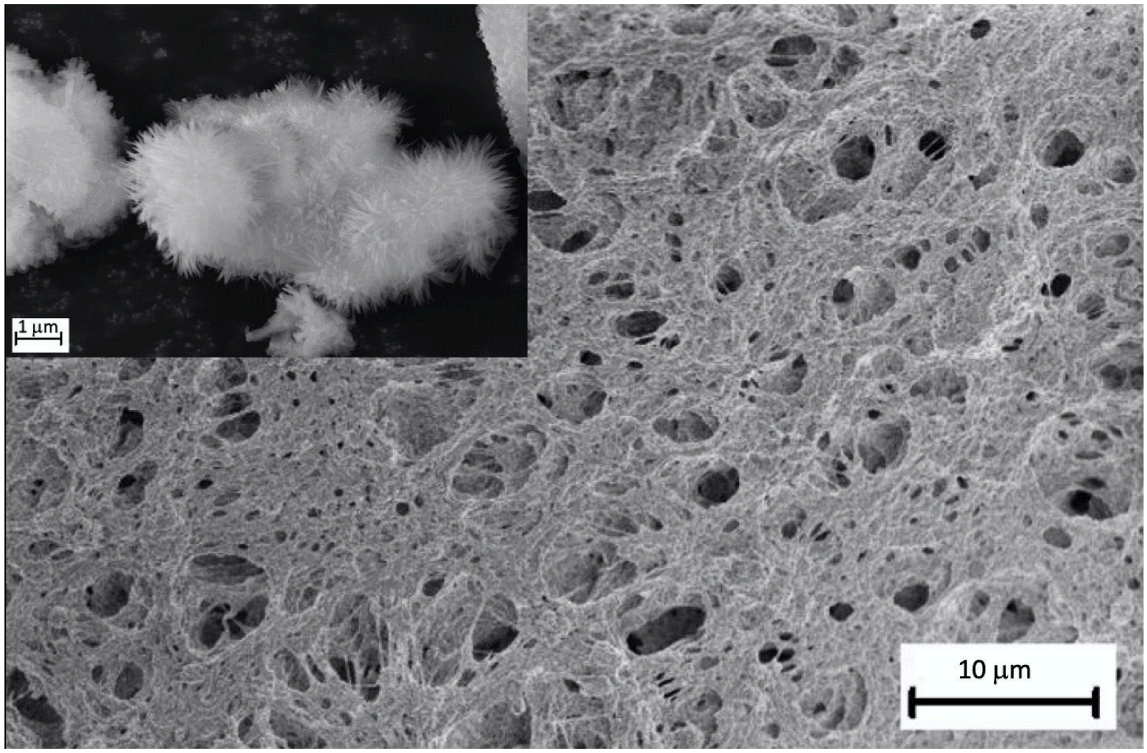

Figure 2. SEM micrograph of the M67 membrane surface. Inset: SEM micrograph of the pristine Al-fumarate showing its aggregated needle-like crystal morphology.

3.2. Adsorption/Desorption Behavior

Nitrogen adsorption/desorption isotherms at 77 K (Figure 3A) were collected to evaluate the MOF microporosity in the composite. The M67 membrane exhibits a type I + II isotherm closely following the shape of pristine Al-fumarate. The normalized BET surface area was 890 m^2/g_{MOF}, corresponding to about 90% retention of the pristine MOF surface area (1010 m^2/g). The HK pore size distribution is centered at 2.54 Å for both the pristine MOF and the composite, confirming that the microporous structure is fully preserved. A cumulative mesoporous volume of 0.19 cm^3/g can be calculated from a BJH analysis, with a maximum of the distribution at 3.8 nm; as already reported [21], this mesoporosity is attributable to partial aggregation of the dispersed particles.

Water vapor adsorption and desorption isotherms of the M67 membrane were measured at 50 °C (Figure 3B). The membrane exhibits the characteristic Type V S-shape typical of Al-fumarate, confirming that the MOF retains most of its intrinsic adsorption properties within the polymer matrix. The Type V isotherm originates from a two-stage mechanism. At low RH (<0.2), water molecules coordinate to the open Al^{3+} sites of Al-fumarate via Lewis interactions. At intermediate RH, cooperative hydrogen bonding between adsorbed water and the fumarate linkers promotes water clustering within the active sites, producing the steep S-shaped uptake. At higher RH (>0.6), the pores approach saturation and the uptake plateaus. The preservation of this mechanism in M67 indicates that the PVDF-HFP

matrix does not hinder access to the active sites of MOF, in agreement with the BET and HK results. The water uptake at membrane saturation ($P/P_0 \approx 0.8$) is approximately 0.25 kg_w/kg_{ads}, corresponding to 0.37 kg_w/kg_{ads} normalized to the MOF content, and represents about 90% of the pristine Al-fumarate capacity. Notably, the hysteresis between adsorption and desorption branches is negligible, indicating a trivial contribution from capillary force. Water is readily adsorbed/desorbed for minimal changes in relative humidity, enabling energy-efficient regeneration with minimal thermal input. The adsorption kinetics of the M67 membrane are remarkably fast, reaching the saturation plateau within a few tens of seconds at 50 °C, with equally rapid desorption, confirming excellent kinetic reversibility. This behavior can be attributed to a low energy barrier for water adsorption and desorption, and to a reduced mass-transfer resistance within the porous membrane. The hydrophobic nature of the PVDF-HFP matrix is further confirmed by contact angle measurements (~120°), which prevent liquid water accumulation by capillary condensation and leave the MOF pores fully accessible for vapor adsorption.

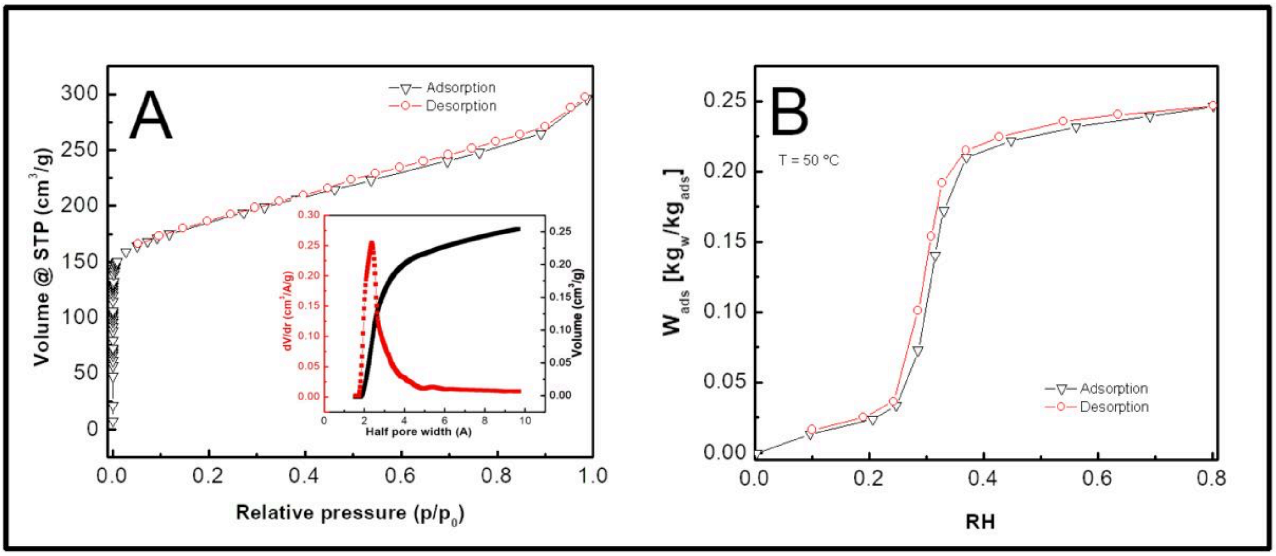

Figure 3. (**A**) N_2 adsorption/desorption isotherms at 77 K of the M67 MMM. The inset shows the HK pore size distribution (left axis, red) and cumulative pore volume (right axis, black). (**B**) Water vapor adsorption/desorption isotherms at 50 °C of the M67 MMM.

Finally, the performance of the M67 membrane was evaluated under representative HVAC operating conditions (process air at 30 °C, 40% RH; regeneration air at 70 °C, 10% RH) and compared with that of conventional silica gel (Figure 4). The MMM exhibits a significantly higher water uptake (0.22 kg_w/kg_{ads}) compared to silica gel (0.14 kg_w/kg_{ads}), representing a 57% improvement. This difference can be rationalized by the distinct adsorption mechanisms of the two materials. Silica gel relies primarily on capillary condensation in mesopores, a process that becomes significant only at higher relative humidity and requires higher regeneration temperatures to evaporate the condensed water. In contrast, Al-fumarate adsorbs water through site-specific coordination to Al^{3+} centers and subsequent clustering in micropores, which is energetically more favorable and occurs efficiently even at moderate RH. Under the tested HVAC operating conditions (process air at 30 °C, 40% RH), the MMM operates in the favorable site-specific adsorption regime, whereas silica gel is still far from capillary saturation. This mechanistic advantage translates into a higher working capacity and lower regeneration energy demand.

This superior adsorption capacity, combined with the negligible hysteresis and rapid kinetics discussed above, positions the MMM as an effective alternative to traditional desiccants for energy-efficient dehumidification. The developed MMM thus offers superior

water adsorption performance compared to conventional desiccants, with the added advantage of negligible hysteresis—characteristics that translate directly into energy savings in HVAC applications, where the regeneration step typically accounts for a significant portion of the operating cost. By embedding the MOF particles in a flexible, mechanically stable polymer matrix, the membrane enables the realization of a fixed-bed desiccant module that can be integrated into existing HVAC and other drying systems.

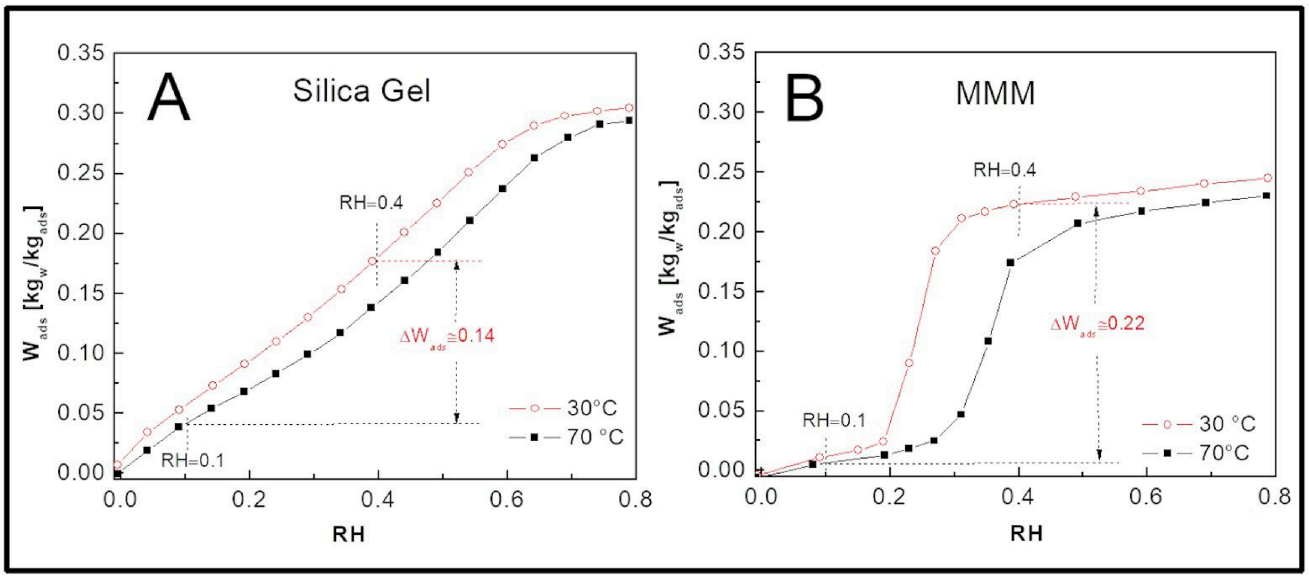

Figure 4. Comparison of water uptake under representative HVAC operating conditions (process air: 30 °C, 40% RH; regeneration air: 70 °C, 10% RH) between (**A**) conventional silica gel and (**B**) MMM (M67 membrane). The MMM (**B**) shows a 57% higher uptake than silica gel (**A**) (0.22 vs. 0.14 kgw/kgads) The dashed lines indicate the working capacity difference (ΔW_ads) between adsorption and desorption.

4. Conclusions

We developed an Al-fumarate/PVDF-HFP Mixed Matrix Membrane with 67 wt% MOF loading by solution casting. The M67 membrane retains ~90% of pristine MOF surface area and water adsorption capacity, preserves the Type V isotherm with negligible hysteresis, and shows good mechanical stability and hydrophobicity. Under HVAC conditions, it outperforms silica gel by 57% (0.22 vs. 0.14 kg_w/kg_{ads}). This improvement is attributed to the site-specific coordination of water to Al^{3+} sites in Al-fumarate, which is more efficient at low RH than the capillary condensation mechanism dominating in silica gel. The negligible hysteresis observed for the MMM further confirms that regeneration is not limited by capillary water retention, unlike conventional desiccants. The MMM addresses powder handling limitations, enabling fixed-bed desiccant modules for scalable, energy-efficient dehumidification. Ongoing work focuses on engineering a membrane-based module and validating it under real conditions.

Author Contributions: Conceptualization, M.P. and F.P.; methodology, M.P.; validation, A.F., C.S., S.D.A., F.P., and M.P.; formal analysis, M.P.; investigation, A.F., C.S., S.D.A., F.P., and M.P.; data curation, M.P., F.P.; writing—original draft preparation, M.P.; writing—review and editing, A.F., C.S., S.D.A., F.P., and M.P.; visualization, M.P.; supervision, M.P.; project administration M.P. All authors have read and agreed to the published version of the manuscript.

Funding: This research received no external funding.

Institutional Review Board Statement: Not applicable. This study did not involve humans or animals.

Informed Consent Statement: Not applicable. This study did not involve humans.

Data Availability Statement: The data presented in this study are available on request from the corresponding author.

Conflicts of Interest: The authors declare no conflict of interest.

References

1. Zhou, H.C.; Long, J.R.; Yaghi, O.M. Introduction to Metal-Organic Frameworks. *Chem. Rev.* **2012**, *112*, 673–674. [CrossRef]
2. Safaei, M.; Foroughi, M.M.; Ebraimpoor, N.; Jahani, S.; Omidi, A.; Khatami, M. A review on metal-organic frameworks: Synthesis and applications. *TrAC Trends Anal. Chem.* **2019**, *118*, 401–425. [CrossRef]
3. Firooz, S.K.; Armstrong, D.W. Metal-organic frameworks in separations: A review. *Anal. Chim. Acta* **2022**, *1234*, 340208. [CrossRef]
4. Duan, Y.; Li, L.; Shen, Z.; Cheng, J.; He, K. Engineering Metal-Organic-Framework (MOF)-based Membranes for Gas and Liquid Separation. *Membranes* **2023**, *13*, 480. [CrossRef]
5. Haruna, A.; Zango, Z.U.; Tanimu, G.; Izuage, T.; Musa, S.G.; Garba, Z.N.; Merican, Z.M.A. A critical review on recent trends in metal-organic framework-based composites as sustainable catalysts for environmental applications. *J. Environ. Chem. Eng.* **2024**, *12*, 113542. [CrossRef]
6. Kim, H.; Yang, S.; Rao, S.R.; Narayanan, S.; Kapustin, E.A.; Furukawa, H.; Usmans, A.S.; Yaghi, O.M.; Wang, E.N. Water harvesting from air with metal-organic frameworks powered by natural sunlight. *Science* **2017**, *356*, 430–434. [CrossRef]
7. Fan, W.; Wang, K.Y.; Welton, C.; Feng, L.; Wang, X.; Liu, X.; Li, Y.; Kang, Z.; Zhou, H.C.; Wang, R.; et al. Aluminum metal-organic frameworks: From structures to applications. *Coord. Chem. Rev.* **2023**, *489*, 215175. [CrossRef]
8. Fu, Y.; Yang, D.; Chen, Y.; Shi, J.; Zhang, X.; Hao, Y.; Zhang, Z.; Sun, Y.; Zhang, J. MOF-Based Active Packaging Materials for Extending Post-Harvest Shelf-Life of Fruits and vegetables. *Materials* **2023**, *16*, 3406. [CrossRef]
9. Yang, Y.; Hu, W.; Li, A.; An, Y.; Xu, W.; Gao, H.; Huang, D.; Zou, R. Metal-organic frameworks for stabilizing metal anodes in advanced rechargeable batteries. *Coord. Chem. Rev.* **2026**, *550*, 217407. [CrossRef]
10. Kundu, S.; Swaroop, A.K.; Selvaraj, J. Metal-Organic Framework in Pharmaceutical Drug delivery. *Curr. Top. Med. Chem.* **2023**, *23*, 1155–1170. [CrossRef]
11. Bellocchi, S.; Guizzi, G.L.; Manno, M.; Pentimalli, M.; Salvatori, M.; Zaccagnini, A. Adsorbent materials for low-grade waste heat recovery: Application to industrial pasta drying processes. *Energy* **2017**, *140*, 729–745. [CrossRef]
12. Guizzi, G.L.; Manno, M.; Zaccagnini, A.; Salvatori, M.; Bellocchi, S. *Sistema Dimostrativo Steam per il Recupero Energetico da Cascami Termici a Bassa Temperatura. Prove Cicliche di Lunga Durata e con Cicli Parziali*; Report RdS/PAR2018/078; ENEA: Roma, Italy, 2018.
13. Pentimalli, M.; Aliboni, A.; Bellusci, M.; La Barbera, A.; Padella, F.; Pilloni, L.; Varsano, F. *Sviluppo di un Composito a Matrice Polimerica ad alto Caricamento di MOF. Prove di Fattibilità e Valutazioni Esplorative*; Report RdS/PAR 2018/077; ENEA: Roma, Italy, 2018.
14. Cai, R.; Wang, Y.; Chen, J.; Li, Z. From metal–organic framework powders to shaped solids: Recent developments and challenges. *Coord. Chem. Rev.* **2021**, *2*, 7139–7186. [CrossRef]
15. Dechnik, J.; Gascon, J.; Doonan, C.J.; Janiak, C.; Sumby, C.J. Mixed-Matrix Membranes. *Angew. Chem. Int. Ed.* **2017**, *56*, 9292–9310. [CrossRef]
16. Jani, D.B.; Mishra, M.; Sahoo, P.K. Solid desiccant air conditioning – A state of the art review. *Renew. Sustain. Energy Rev.* **2016**, *60*, 1451–1469. [CrossRef]
17. Lanceros-Méndez, S.; Costa, C.M. Poly(vinylidene fluoride) (PVDF) and its copolymers for energy applications. In *Polymer-Based Materials for Energy Applications*; Elsevier: Amsterdam, The Netherlands, 2021.
18. Pentimalli, M.; De Antonellis, S.; Giuffrida, M.F.; Martinelli, A.; Pilloni, L.; Padella, F. Al-fumarate/PVDF-HFP Mixed matrix membrane for water vapor adsorption in industrial drying processes. *Mater. Sci. Eng. B* **2025**, *312*, 118663. [CrossRef]
19. Lutterotti, L.; Matthies, S.; Wenk, H.-R. *MAUD (Material Analysis Using Diffraction)*, version 2.999; University of Trento: Trento, Italy, 2025. Available online: https://maud.radiographema.eu (accessed on 19 July 2026).
20. Perbet, M.; Aumond, T.; Collomb, C.; Daniel, C.; Imaz, I.; Pena, G.; Maspoch, D.; Michon, T.; Morales-Ospino, R.; Fierro, V.; et al. Upscaled Al-Fumarate Synthesis and Shaping by Spray Drying. *Ind. Eng. Chem. Res.* **2025**, *64*, 6541–6549. [CrossRef]
21. Lipsa, L.; Rajput, S.; Parida, S.; Ghosh, S.P.; Verma, S.K.; Gupta, S. Influence of Hot-Press Temperature on β-Phase Formation and Electrical Properties of Solvent-Casted PVDF-HFP Co-Polymer Films Prepared from Two Different Solvents: A Comparison Study. *Macromol. Chem. Phys.* **2023**, *224*, 2300204. [CrossRef]

Disclaimer/Publisher's Note: The statements, opinions and data contained in all publications are solely those of the individual author(s) and contributor(s) and not of MDPI and/or the editor(s). MDPI and/or the editor(s) disclaim responsibility for any injury to people or property resulting from any ideas, methods, instructions or products referred to in the content.